Boundary-Layer Meteorol (2016) 158:489–499
DOI 10.1007/s10546-015-0099-4

NOTES AND COMMENTS

Surface-Parallel Sensor Orientation for Assessing Energy Balance Components on Mountain Slopes

P. Serrano-Ortiz[1,2] · E. P. Sánchez-Cañete[2,3] · F. J. Olmo[2,4] · S. Metzger[5,6] · O. Pérez-Priego[7] · A. Carrara[8] · L. Alados-Arboledas[2,4] · A. S. Kowalski[2,4]

Received: 12 June 2015 / Accepted: 13 October 2015 / Published online: 28 October 2015

Abstract The consistency of eddy-covariance measurements is often evaluated in terms of the degree of energy balance closure. Even over sloping terrain, instrumentation for measuring energy balance components is commonly installed horizontally, i.e. perpendicular to the geo-potential gradient. Subsequently, turbulent fluxes of sensible and latent heat are rotated perpendicular to the mean streamlines using tilt-correction algorithms. However, net radiation (R_n) and soil heat fluxes (G) are treated differently, and typically only R_n is corrected to account for slope. With an applied case study, we show and argue several advantages of installing sensors surface-parallel to measure surface-normal R_n and G. For a 17 % south-west-facing slope, our results show that horizontal installation results in hysteresis in the energy balance closure and errors of up to 25 %. Finally, we propose an approximation to estimate the surface-normal R_n, when only vertical R_n measurements are available.

Keywords Energy balance closure · Hysteresis · Net radiation · Soil heat flux · Sloping terrains

✉ P. Serrano-Ortiz
penelope@ugr.es

1 Departamento de Ecología, Universidad de Granada, 18071 Granada, Spain

2 Andalusian Institute for Earth System Research (CEAMA-IISTA), Universidad de Granada, 18006 Granada, Spain

3 B2 Earthscience, Biosphere 2, University of Arizona, Tucson, AZ 85721, USA

4 Departamento de Física Aplicada, Universidad de Granada, 18071 Granada, Spain

5 National Ecological Observatory Network (NEON), Boulder, USA

6 Institute for Arctic and Alpine Research, University of Colorado, Boulder, USA

7 Department of Biogeochemical Integration, Max Planck Institute for Biogeochemistry, 07745 Jena, Germany

8 Fundación Centro de Estudios Ambientales del Mediterráneo (CEAM), 46980 Valencia, Spain

1 Introduction

The measurement of turbulent fluxes in varying environments is an approach that is used for assessing and forecasting global warming (Kaminski et al. 2012; Koffi et al. 2013). Thus, eddy-covariance towers have proliferated around the world in the last two decades (FLUXNET tower network; Baldocchi et al. 2001). Since ideal sites are rarely found worldwide, there was a great need to extend the applicability of the eddy-covariance method to situations over non-ideal (or "complex") terrain. Different studies even concluded that the eddy-covariance method can be used over sloping terrain to evaluate energy and CO_2/H_2O fluxes of whole ecosystems (Hammerle et al. 2007; Hiller et al. 2008). However, general problems of the eddy-covariance method are aggravated by sloping terrain. Both the error induced by neglecting the vertical and horizontal advective fluxes (Aubinet et al. 2003, 2005) and the underestimation of nighttime ecosystem respiration during stable conditions (Gu et al. 2005; Aubinet 2008) depend critically on slope, although such problems are less pronounced over short vegetation.

One of the most commonly used methods for evaluating the consistency of eddy-covariance turbulent flux measurements is to assess closure of the energy balance (Wilson et al. 2002; Stoy et al. 2013). This quality control criterion for eddy-covariance measurements consists of comparing the sum of the latent (LE) and sensible (H) heat fluxes, measured with the eddy-covariance method, to the available energy consisting of net radiation (R_n) minus the soil heat flux (G). According to the first law of thermodynamics, incoming and outgoing energy components must balance. This independent assessment of eddy-covariance measurement reliability has been evaluated for many FLUXNET sites with a mean imbalance on the order of 20% (Wilson et al. 2002). The reasons for the general imbalance remain unclear and are under discussion (Foken 2008; Leuning et al. 2012; Stoy et al. 2013), and turbulent fluxes are often considered "acceptable" when the energy balance residual does not exceed 30%. Over sloping terrain, the energy-budget quality control yields results comparable to those for sites located in near flat terrain (Hammerle et al. 2007; Hiller et al. 2008; Etzold et al. 2010). In the following, we focus on ecosystem-scale exchanges over a mountain slope that is quasi-uniform across and beyond the source area (footprint) of the flux measurements. That is, we focus on the effect of the average slope over scales of hectares on the energy balance. Smaller undulations that can even exist within flat terrain (such as ploughed farmlands) are not the subject of our study and are addressed elsewhere (Wohlfahrt and Tasser 2014).

Overall, the goal of an energy balance study must be to represent all contributing terms in the same way that they influence the exchange surface. This can be achieved by minimizing the incident angle between a contributing term and its measurement regardless of the exchange surface orientation. Atmospheric turbulence results in down-gradient transport by turbulent diffusion, with the "exchange" coordinate of the scalar flux being perpendicular to the streamlines/surface. For radiation components, both the irradiance and emittance relevant to the surface are clearly in the normal direction, irrespective of the geopotential gradient (this is why solar panels are not installed horizontally). Such net radiative effects also establish isotherms parallel to the surface and soil temperature gradients in the surface-normal direction, which is therefore the relevant direction to measure G.

Over sloping sites, eddy-covariance systems are typically installed horizontally and the resulting fluxes H and LE are subsequently rotated perpendicular to the mean streamlines. However, the R_n and G terms contributing to the energy balance are treated differently. Net radiometers are installed horizontally, and either (a) no rotation is applied (e.g., Etzold et al.

2010), or (b) the incoming solar radiation component of the net radiation is corrected for the inclination, arguing that this is the most important component contributing to R_n (Matzinger et al. 2003; Hammerle et al. 2007; Hiller et al. 2008; Saitoh et al. 2011). Oftentimes no information is provided on the alignment of the R_n and G sensors.

Here, we examine the advantages of installing the net radiometer and soil heat flux instruments parallel to the average slope. Section 2 provides information on the study site and the sensor deployments. In Sect. 3, we present the case study results of horizontal *vs.* parallel sensor installations, and propose an approximation to estimate surface-normal R_n, when only vertical R_n measured with horizontally oriented (i.e., level) sensors is available. Finally, in Sects. 4 and 5 we discuss our findings and provide concluding recommendations.

2 Methods

2.1 Site Description

The experimental part of the study was conducted in the Sierra Nevada National Park in south-eastern Spain (36°58′3.68″N; 3°28′37.04″W, 2320 m a.s.l.; Fig. 1). Vegetation consists of grass and forbs (*Genista versicolor, Festuca spp.* and *Sessamoides prostata*, dominant species) recovering in the wake of a 2005 wildfire. Given the short vegetation and the aerodynamically simple surface, the contribution of air storage to net exchanges is very small and thus neglected (Suyker and Verma 2001; Kowalski et al. 2003). An eddy-covariance tower was installed in 2009 over an averaged slope of 17 % of south-west (255°) aspect. Previous studies showed that fluxes typically originate from source areas within approximately 300 m of the tower (Serrano-Ortiz et al. 2011).

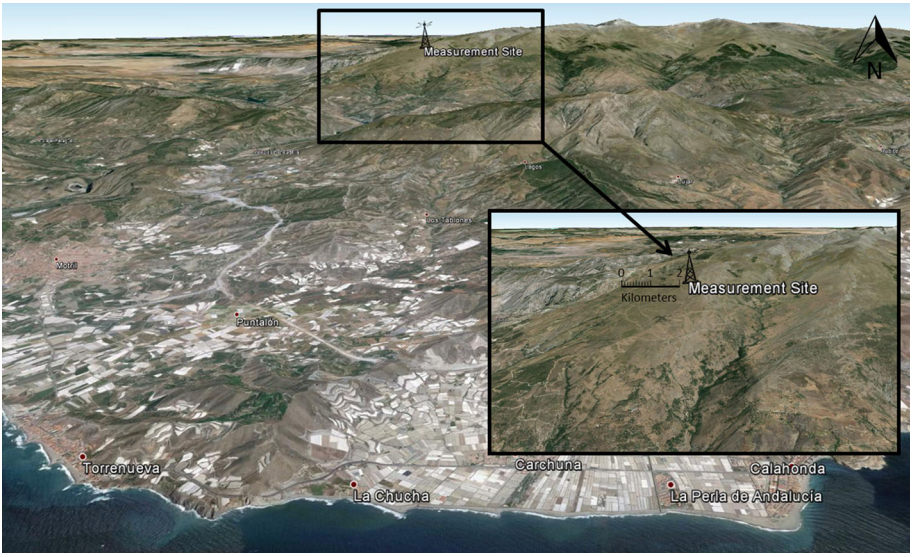

Fig. 1 Measurement site on the south-western slopes of the Sierra Nevada National Park, Spain (tower not to scale.). *Source* Google Earth, 36°58′3.68″N; 3°28′37.04″W, image: Landsat, imagery date August 4 2012, accessed November 9 2014

2.2 Sensor Deployments

The following analyses were performed on data from 7 July to 20 August 2010, with 34 days under cloud-free conditions and 10 partially cloudy days; no fully overcast conditions occurred. During this period the eddy-covariance tower provided turbulent exchanges of energy between the surface and the atmosphere. Sensible (H) and latent (LE) heat fluxes were calculated from fast-response (10 Hz) instruments (infrared gas analyzer Li-7500, Lincoln, Nebraska, USA; a three-axis sonic anemometer model 81000 (R.M. Young, Traverse City, Michigan, USA), mounted horizontally so that "w" represents the vertical wind, with a valid operating range for attack angle in the range $\pm 60°$) mounted atop a 6-m tower.

Means, variances and covariances were calculated for 30-min periods following the Reynolds rules, and eddy-flux corrections for density perturbations (Webb et al. 1980) and tests for stationarity and turbulence development were applied using the EddyPro 5.1.1 software. The stationarity test compares the covariances determined for the 30-min period and for shorter intervals within this period (usually 5 min). A time series is considered to be steady state if the difference between both covariances is less than 30 % (Mauder and Foken 2004). The turbulence development was tested by using the so-called flux-variance similarity where the ratio of the standard deviation of a turbulent parameter and its turbulent flux (measured parameter) is a function of the stability (modelled parameter). Well developed turbulence can be assumed if the difference between the measured and the modelled parameter is less than 30 % (Mauder and Foken 2004). After applying both tests, the EddyPro 5.1.1 software provides the flag "0" for high quality fluxes (differences <30 % for both test), "1" for intermediate quality fluxes (differences <30 % for one test) and "2" for poor quality fluxes (differences >30 % for both tests).

Since no systematic error has been observed for applying different rotation methods over sloped sites (e.g., Turnipseed et al. 2003; Shimizu 2015) and particularly for our experimental site (double rotation vs. planar fit showed no significant differences, data not shown), the double coordinate rotation was used to ensure that the rotated average "w" is zero in the direction normal to the surface. While double rotation of 30-min data is one of the most common methods used, it is frequently cited inadequately: the often-cited McMillen (1988) relied on erroneous equations of Tanner and Thurtell (1969). The correct version was first provided by Kowalski et al. (1997) and is now also frequently cited via Aubinet et al. (2000).

In addition to the turbulent fluxes, available energy was determined by duplicate sensors in two configurations, one parallel to the surface and the other horizontal. For each, a net radiometer (NR Lite, Kipp&Zonen, Delft, Netherlands) was located 2 m above the surface, and two heat-flux plates (HFP01SC, Hukseflux, Delft, Netherlands) were installed at 80-mm depth, with two pairs of soil temperature probes (TCAV, Campbell Scientific, Logan, Utah, USA) at 20- and 60-mm depth, and a water content reflectometer (CS616, Campbell Scientific, Logan, Utah, USA) at 40-mm depth. The soil heat flux (G) was calculated by adding the measured heat flux at a fixed depth (80 mm) under bare soil to the energy stored in the layer above the heat-flux plates, based on the specific heat capacity of the soil and changes in the temperature and soil water content with time (Massman 1992; Domingo et al. 2000). Finally, the incident and reflected photosynthetic photon flux densities (PPFD) were measured by quantum sensors (Li-190, Lincoln, Nebraska, USA) to identify the partially cloudy days and estimate the surface albedo.

2.3 Modelling

Following Olmo et al. (1999), the surface-normal R_n was modelled based on vertical R_n measurements. First, vertical daytime R_n values were converted to global irradiance (R_g), defined as the total amount of shortwave radiation (direct + diffuse; W m^{-2}) received from above at the surface (Iqbal 1983), using the linear relationship between R_n and R_g evaluated by Alados et al. (2003) for semi-arid sites,

$$R_n = a R_g + b, \tag{1}$$

where $a = 0.709$ and $b = -25.4$ W m^{-2}.

Secondly, the daytime surface-normal R_g was modelled following Olmo et al. (1999)

$$R_{g\psi} = R_g \exp\left(-k_t \left(\psi^2 - \theta_z^2\right)\right) F_c, \tag{2}$$

where $R_{g\psi}$ is the global irradiance at the inclined surface, R_g is the global irradiance on the horizontal surface, ψ is the angular distance (in radians) from the surface normal to the sun's position, θ_z denotes the solar zenith angle, k_t is the clearness index, F_c is a multiplying factor to take into account anisotropic reflections.

The angular distance ψ can be evaluated as follows,

$$\cos\psi = \sin\alpha \sin\alpha_s + \cos\alpha \cos\alpha_s \cos(\varphi_s - \varphi), \tag{3}$$

where α is the angle of the slope (surface elevation) with respect to the horizontal surface, α_s is the sun elevation angle with respect to the horizontal surface, φ_s is the sun azimuth and φ the surface azimuth (Fig. 2).

The clearness index can be evaluated as follows,

$$K_t = R_g / R_{gext}, \tag{4}$$

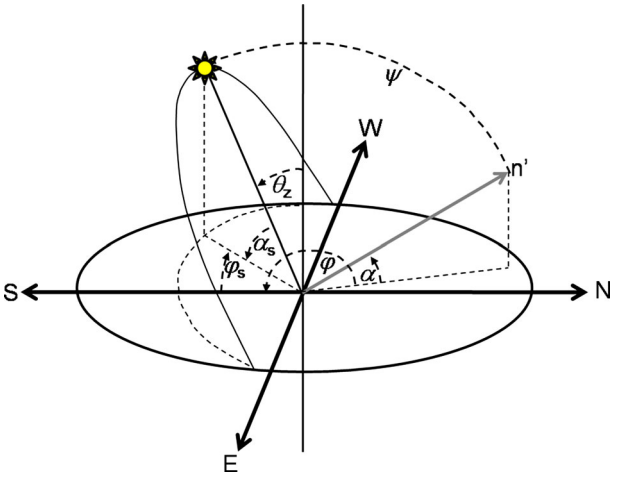

Fig. 2 Sketch of the angles involved in the radiation model. Angular distance (in radians) from the surface normal (n') to the sun's position (ψ); solar zenith angle (θ_z); angle of the slope (surface elevation) with respect to the horizontal surface (α), sun elevation angle respect to the horizontal surface (α_s), sun azimuth (φ_s), surface azimuth (φ)

where R_{gext} is the extraterrestrial irradiance calculated as follows (Iqbal 1983),

$$R_{gext} = I_{sc}(r_0/r)^2 \cos\theta_z, \tag{5}$$

where I_{sc} is the solar constant (1367 W m^{-2}), r_o is the average sun-earth distance and r is the real sun-earth distance according to day of year.

Concerning the anisotropic correction factor, F_c, we have tested various types of functions and obtained the best agreement between the computed and observed radiation values as follows,

$$F_c = \sin\psi(1/(0.55 - \rho)), \tag{6}$$

where ρ is the surface albedo, approximated as the ratio of the average daytime reflected to incident PPFD for the studied period ($\rho = 0.12$).

Thirdly, the obtained results were converted into surface-normal R_n values ($R_{n\psi}$), using again the site-specific linear regression (1). Finally, the nighttime values of surface-normal R_n were directly modelled as

$$R_{n\psi} = R_n \, cos\alpha_s. \tag{7}$$

In contrast to the R_n measurements, the vector components of the soil heat flux are not known. Also, unlike the turbulence sensors the soil heat-flux plate measures only along a single axis. Consequently, no correction was attempted for transforming vertical G into a surface-normal coordinate.

3 Results

Data are reported using Coordinated Universal Time (UTC), which leads local solar time at this site by less than 15 min.

For our study case, vertical R_n and G measured with horizontal sensor orientation underestimate available energy due to the slight southern aspect of the slope, with the expected delay in the maxima due to the predominantly western aspect (Fig. 3a). Significant differences between morning and afternoon values and daily totals of R_n and G were measured comparing both orientations. The radiometer installed horizontally overestimated morning R_n by around 100 W m^{-2} and underestimated afternoon values by around 150 W m^{-2}, resulting in 21 and 16 % underestimations of the daily means under cloud-free and partially cloudy conditions respectively (Fig. 3). Similarly, horizontally installed soil heat-flux plates overestimated morning values by around 25 W m^{-2} and underestimated afternoon values by 40 W m^{-2}, leading to an overall underestimation of 13 % in the daily totals under cloud-free conditions; no underestimation was observed under partially cloudy conditions (Fig. 3c).

This results in a clear hysteresis in energy balance closure when vertical R_n and G values from horizontal sensors are used (Figs. 4a, 5a). Maximum values of vertical R_n and G were measured at noon, whereas for rotated H and LE the peaks occurred in late afternoon (Fig. 5a). The situation is resolved when sensors are installed parallel to the slope, measuring surface-normal R_n and G. *P*eak values of all components of the energy balance occurred in late afternoon, in accordance with the south-western aspect of the slope (Fig. 5f), improving both the slope (from 1.20 to 1.06; Fig. 4f) and the explained variance (R^2 from 0.83 to 0.99; Fig. 4f) of the linear least-squares regression. When vertical G is measured with horizontal sensor orientation (Fig. 5c), the energy balance closure (regression slope) does not change substantially, but scatter of around 100 W m^{-2} increases (Fig. 4c). When the modelled

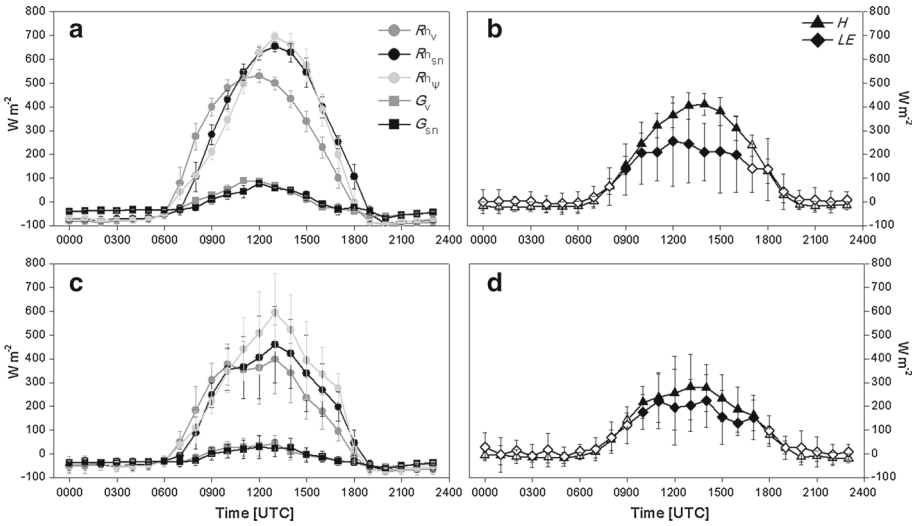

Fig. 3 Daily patterns of the energy balance components under cloud-free (**a**, **b**) and partially cloudy (**c**, **d**) conditions. Vertical radiation (R_n) and soil heat flux (G) measured with horizontal sensor orientation (*subscript* "v"; *dark gray symbols*), surface-normal R*n* and *G* measured with surface-parallel sensor orientation (*subscript* "sn"; *black symbols*) and modelled surface-normal R_n (*subscript* "ψ"; *light gray circles*) for **a** and **c**. Surface-normal sensible (H) and latent heat (LE) fluxes for **b** and **d**. Each *point* represents the hourly ensemble value for the fourth week of August 2010 (±SD). *Open symbols* for **b** represent points with <60 % of data with quality flag "0" following Mauder and Foken (2004)

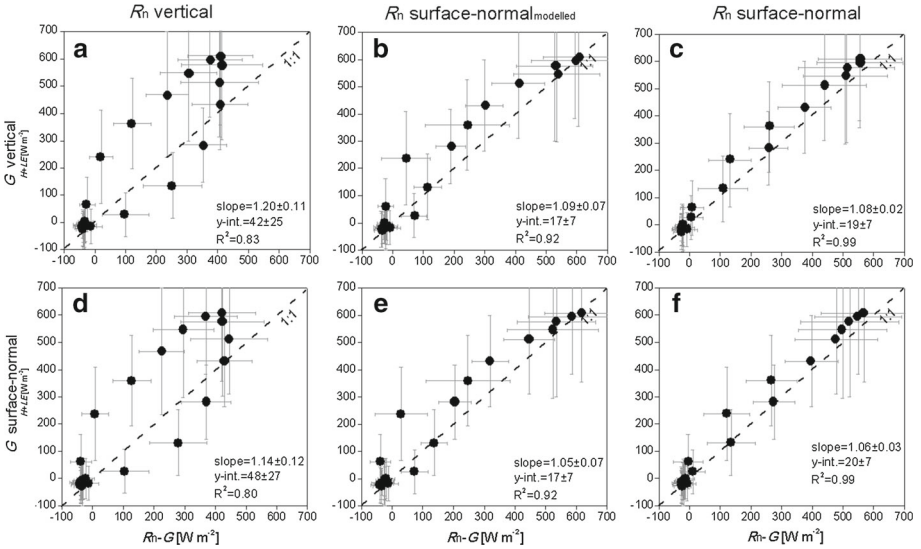

Fig. 4 Energy balance closure for different energy-sensor combinations: net radiation (R_n), soil heat flux (G) and surface-normal sensible (H) and latent (LE) heat fluxes. Each *point* represents the hourly ensemble value ($H + LE$ *vs.* $R_n + G$) for the entire measured period combining cloud-free and partially cloudy days (±standard deviation). Information about the slope, y-intercept and R^2 is provided

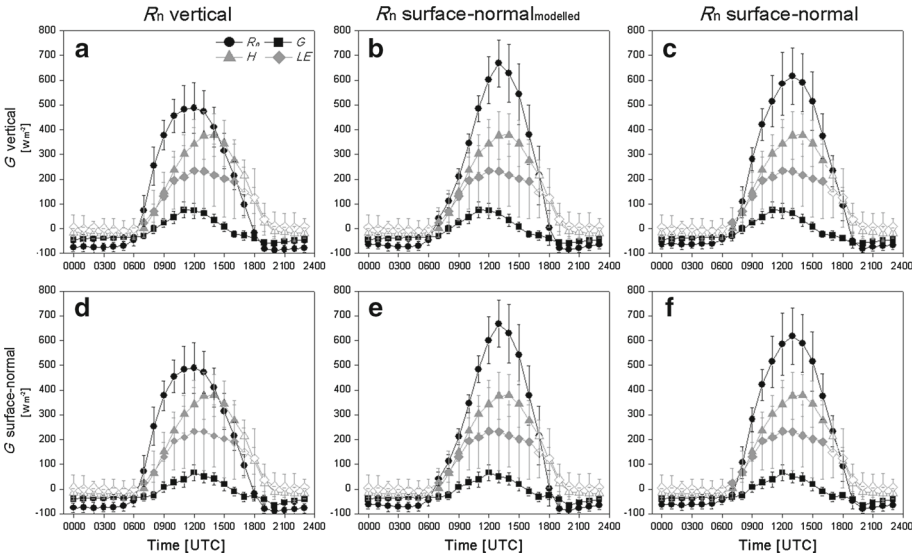

Fig. 5 Daily patterns of the energy balance components for different energy sensor combinations:net radiation (R_n), soil heat flux (G) and surface-normal sensible (H) and latent (LE) heat fluxes. Each *point* represents the hourly ensemble value of the different energy components for the entire measured period combining cloud-free and partially cloudy days (±standard deviation). *Open circles* represent points with <60 % of data with quality flag "0" following Mauder and Foken (2004)

surface-normal R_n is used (Fig. 5b and e), the regression fit is also improved ($R^2 = 0.92$; Fig. 4b and e). Note that, despite the good match between measured and modelled surface-normal R_n (slope $= 1.009 \pm 0.005$, y-intercept $= -2 \pm 1$, $R^2 = 0.96$; $n = 1983$), the comparison of daily patterns shows clear mismatches at sunrise, sunset and midday (Fig. 3). Under cloud-free conditions (Fig. 3a) modelled surface-normal R_n overestimated sunrise and midday values by around 70 W m^{-2} and similarly underestimated sunset values. Under partially cloudy conditions (Fig. 3c), modelled surface-normal R_n yielded clearly overestimated values from 0900 to 1700 UTC by up to 135 W m^{-2}. This results in a deviation from the energy balance closure 1:1 line between 100 and 300 W m^{-2} when considering the whole database (Fig. 4b, e), and 6 % underestimation and 20 % overestimation in the daily mean for sunny and partially cloudy days respectively (Fig. 3a, c).

4 Discussion

Our case study confirms improved energy balance closure when both the net radiometer and soil heat-flux instruments were installed parallel to the slope compared to other configurations, such as horizontal or modelled normal-surface R_n. For the case of G, with a modest contribution to the energy balance, parallel installation did not substantially improve the slope, but did reduce the scatter. It needs to be considered that G measurements only represent their immediate environment (of order 0.01 m^2) whereas radiation and turbulent flux measurements represent areas of order 100 and 1000 m^2, respectively, for these measurement heights. Hence, for representing a spatial scale more comparable to the radiation and flux measurements, a population of soil plates placed parallel to the average slope is required.

Since R_n represents more than 70 % of available energy, it is commonly accepted by the FLUXNET community that radiometers be installed horizontally and to approximate surface-normal R_n following trigonometric corrections in post-processing, but to neglect the effect of the slope on G (Hammerle et al. 2007; Hiller et al. 2008; Zitouna-Chebbi et al. 2012). If such an approximation is to be performed reliably, not only net radiometers but also pyranometers should be installed to distinguish the total, direct and diffuse shortwave radiation components. In such a way, direct shortwave radiation can be easily corrected for slope effects knowing the azimuthal and elevation angles, latitude and surface inclination (Garnier and Ohmura 1968; Whiteman et al. 1989). Since direct shortwave radiation represents 60 to 80 % of R_n for mid-latitudes, and is the component most affected by slope effects (Holst et al. 2005), such post-processing correction typically yields acceptable results. However, according to Oliver (1992), under partially cloudy conditions, information about cloud cover and opacity is required and the correction quickly becomes either complex or inaccurate. Moreover, not only the direct but also the reflected shortwave radiation component (from 5 to 15 % of total R_n) is affected by the slope (Holst et al. 2005). Additionally, our results show that, under cloud-free conditions, approximating surface-normal R_n is justified when stations measure only R_n and not its components. However, under partially cloudy conditions the model clearly overestimates R_n. Unfortunately, fully overcast conditions were lacking during our experiment, and we cannot evaluate the model performance on cloudy days. Furthermore, a site-specific linear regression relationship is required as an intermediate step to convert measured R_n into global irradiance and vice versa.

While in the immediate air layer above an exchange surface, net transport is down-gradient, i.e. surface-normal, there are also relevant cases for examining the vertical exchange of heat: with increasing distance from the exchange surface, some types of atmospheric flows are dominated by buoyancy. In this case the relevant direction of transport is vertical, following the geopotential gradient. For example, when considering atmospheric stability, the vertical exchange of heat (or actually: buoyancy) must be considered. This implies the need to consider vertical buoyancy fluxes when calculating the Richardson number, for example, irrespective of surface orientation.

5 Conclusion and Recommendations

For energy balance studies the transport direction of interest is surface-normal. Consequently, for assessing the energy balance over a sloping surface without complex local topography or undulations, we recommend installing the net radiometer and soil heat flux plates parallel to the average slope. For other uses, such as validation of regional numerical models using the energy fluxes measured at the ecosystem scale, spatial aggregation beyond differing definitions of the exchange direction needs to be considered. Equally important, slope and aspect lead to distinct differences in the ecosystem types, necessitating a careful evaluation of spatial representativeness of the measured fluxes.

Acknowledgments We thank the following for their critical opinions and valuable comments: Edward Ayres, Robert Clement, Thomas Foken, Hongyan Luo, Harry McCaughey, Natchaya Pingintha-Durden, and Jielun Sun. This research was funded in part by the Andalusia Regional Government through projects P12RNM-2409 and P10-RNM-6299, by the Spanish Ministry of Economy and Competitiveness though projects CGL2010-18782, CGL2014-52838-C2-1-R (GEISpain) and CGL2013-45410-R; and by European Community's Seventh Framework Programme through INFRA-2010-1.1.16-262254 (ACTRIS), INFRA-2011-1-284274 (InGOS) and PEOPLE-2013-IOF-625988 (DIESEL) projects. The National Ecological Observatory Network is a project sponsored by the National Science Foundation and managed under cooperative agreement by NEON, Inc. This

material is based upon work supported by the National Science Foundation under the grant DBI-0752017. Any opinions, findings, and conclusions or recommendations expressed in this material are those of the author(s) and do not necessarily reflect the views of the National Science Foundation.

References

Alados I, Foyo-Moreno I, Alados-Arboledas L (2003) Relationship between net radiation and solar radiation for semi-arid shrub-land. Agric For Meteorol 116(3–4):221–227. doi:10.1016/S0168-1923(03)00038-8

Aubinet M (2008) Eddy covariance CO(2) flux measurements in nocturnal conditions: an analysis of the problem. Ecol Appl 18(6):1368–1378. doi:10.1890/06-1336.1

Aubinet M, Grelle A, Ibrom A, Rannik Ü, Moncrieff J, Foken T, Kowalski AS, Martin PH, Berbigier P, Bernhofer CH, Clement R, Elbers J, Granier A, Grünwald T, Morgenstern K, Pilegaard K, Rebmann C, Snijders W, Valentini P, Vesla T (2000) Estimates of the annual net carbon and water exchange of forests: the EUROFLUX methodology. Adv Ecol Res 30:113–173

Aubinet M, Heinesch B, Yernaux M (2003) Horizontal and vertical CO_2 advection in a sloping forest. Boundary-Layer Meteorol 108(3):397–417

Aubinet M, Berbigier P, Berhnofer CH, Cescatti A, Feigenwinter C, Granier A, Grünwald TH, Havrankova K, Beinesch B, Longdoz B, Marcolla B, Montagnini L, Sedlak P (2005) Comparing CO_2 storage and advection conditions at night at different carboeuroflux sites. Boundary-Layer Meteorol 116(1):63–93. doi:10.1007/s10546-004-7091-8

Baldocchi DD, Falge E, Gu L, Olson R, Hollinger D, Running S, Anthoni P, Bernhofer CH, David K, Evans R, Fuentes J, Goldstein A, Katul G, Law B, Lee X, Malhi Y, Meyers Tm Paw UKT, Pilegaard K, Schmid HP, Valentini R, Verma S, Vesala T, Wilson K, Wofsy S (2001) FLUXNET: A new tool to study the temporal and spatial variability of ecosystem-scale carbon dioxide, water vapor, and energy flux densities. Bull Am Meteorol Soc 82:2415–2434. doi:10.1175/1520-0477(2001)082<2415:FANTTS>2.3.CO;2

Domingo F, Villagarcia L, Brenner AJ, Puigdefábregas J (2000) Measuring and modelling the radiation balance of a heterogeneous shrubland. Plant Cell Environ 23:27–38. doi:10.1046/j.1365-3040.2000.00532.x

Etzold S, Buchmann N, Eugster W (2010) Contribution of advection to the carbon budget measured by eddy covariance at a steep mountain slope forest in Switzerland. Biogeoscience 7(8):2461–2475. doi:10.5194/bg-7-2461-2010

Foken T (2008) The energy balance closure problem: an overview. Ecol Appl 18(6):1351–1367. doi:10.1890/06-0922.1

Garnier BJ, Ohmura A (1968) A method of calculating the direct shortwave radiation income of slopes. J Appl Meteorol 7(5):796–800. doi:10.1175/1520-0450(1968)007<0796:AMOCTD>2.0.CO;2

Gu L, Falge EM, Boden T, Baldocchi D, Black TA, Saleska SR, Suni T, Verma SB, Vesala T, Wofsy SC, Xu L (2005) Objective threshold determination for nighttime eddy flux filtering. Agric For Meteorol 128:179–197. doi:10.1016/j.agrformet.2004.11.006

Hammerle A, Haslwanter A, Schmitt M, Bahn M, Tappeiner U, Cernuscas A, Wohlfahrt G (2007) Eddy covariance measurements of carbon dioxide, latent and sensible energy fluxes above a meadow on a mountain slope. Boundary-Layer Meteorol 122(2):397–416. doi:10.1007/s10546-006-9109-x

Hiller R, Zeeman MJ, Eugster W (2008) Eddy-covariance flux measurements in the complex terrain of an alpine valley in Switzerland. Boundary-Layer Meteorol 127(3):449–467. doi:10.1007/s10546-008-9267-0

Holst T, Rost J, Mayer H (2005) Net radiation balance for two forested slopes on opposite sides of a valley. Int J Biometeorol 49(5):275–284. doi:10.1007/s00484-004-0251-1

Iqbal M (1983) Introduction to solar radiation. Academic Press, New York 390 pp

Kaminski T, Rayner PJ, Voßbeck M, Scholze M, Koffi E (2012) Observing the continental-scale carbon balance: assessment of sampling complementarity and redundancy in a terrestrial assimilation system by means of quantitative network design. Atmos Chem Phys 12(16):7867–7879. doi:10.5194/acp-12-7867-2012

Koffi EN, Rayner PJ, Scholze M, Chevallier F, Kaminski T (2013) Quantifying the constraint of biospheric process parameters by CO_2 concentration and flux measurement networks through a carbon cycle data assimilation system. Atmos Chem Phys 13(21):10555–10572. doi:10.5194/acp-13-10555-2013

Kowalski AS, Anthoni PM, Vong RJ, Delany AC, Maclean GD (1997) Deployment and evaluation of a system for ground-based measurement of cloud liquid water turbulent fluxes. J Atmos Ocean Technol 14:468–479

Kowalski S, Sartore M, Burlett R, Berbigier P, Loustau D (2003) The annual carbon budget of a French pine forest (Pinus pinaster) following harvest. Global Change Biol 9(7):1051–1065. doi:10.1046/j.1365-2486.2003.00627.x

Leuning R, van Gorsel E, Massman WJ, Isaac PR (2012) Reflections on the surface energy imbalance problem. Agric For Meteorol 156:65–74. doi:10.1016/j.agrformet.2011.12.002

Massman WJ (1992) Correcting errors associated with soil heat flux measurements and estimating soil thermal properties from soil temperature and heat flux plate data. Agric Forest Meteorol 59(3–4):249–266. doi:10.1016/0168-1923(92)90096-M

Matzinger N, Andretta M, van Gorsel E, Vogt R, Ohmura A, Rotach MW (2003) Surface radiation budget in an Alpine valley. Q J R Meteorol Soc 129(588):877–895. doi:10.1256/qj.02.44

Mauder M, Foken T (2004) Documentation and instruction manual of the eddy-covariance software package TK3. Abt Mikrometeorologie 46, 60 pp

McMillen R (1988) An eddy correlation technique with extended applicability to non-simple terrain. Boundary-Layer Meteorol 43(3):231–245. doi:10.1007/bf00128405

Oliver HR (1992) Studies of surface energy balance of sloping terrain. Int J Climatol 12(1):55–68. doi:10.1002/joc.3370120106

Olmo FJ, Vida J, Castro-Diez Y, Alados-Arboledas L (1999) Prediction of global irradiance on inclined surfaces from horizontal global irradiance. Energy 24(8):689–704. doi:10.1016/S0360-5442(99)00025-0

Saitoh TM, Tamagawa I, Muraoka H, Koizumi H (2011) Energy balance closure over a cool temperate forest in steeply sloping topography during snowfall and snow-free periods. J Agric Meteorol 67(3):107–116. doi:10.2480/agrmet.67.3.4

Serrano-Ortiz P, Marañón-Jiménez S, Reverter BR, Sánchez-Castro EP, Castro J, Zamora R, Kowalski AS (2011) Post-fire salvage logging reduces carbon sequestration in Mediterranean coniferous forest. Forest Ecol Manag 262:2287–2296. doi:10.1016/j.foreco.2011.08.023

Shimizu T (2015) Effect of coordinate rotation systems on calculated fluxes over a forest in complex terrain: a comprehensive comparison. Boundary-Layer Meteorol 156:277–301. doi:10.1007/s10546-015-0027-7

Stoy P, Mauder M, Foken T, Marcolla B, Boegh E, Ibrom A, Altaf Arain M, Arneth A, Aurela M, Bernhofer C, Cescatti A, Dellwik E, Duce P, Gianelle D, van Gorsel E, Kiely G, Knohl A, Margolis H, MmCaughey H, Merbold L, Montagnani L, Papale D, Reichstein M, Saunders M, Serrano-Ortiz P, Sottocornola M, Spano D, Vaccari F, Varlagin A (2013) A data-driven analysis of energy balance closure across FLUXNET research sites: The role of landscape-scale heterogeneity. Agric For Meteorol 171–172:137–152

Suyker AE, Verma SB (2001) Year-round observations of the net ecosystem exchange of carbon dioxide in a native tallgrass prairie. Global Change Biol 7(3):279–289. doi:10.1046/j.1365-2486.2001.00407.x

Tanner BD, Thurtell GW (1969) Research and development technical report: Anemoclinometer measurements of Reynold stress and het transport in the atmopheric surface layer. University of Wisconsin, Wisconsin, Grant Number DA-AMC-28-043-066-G022

Turnipseed AA, Anderson DE, Blanken PD, Baugh WM, Monson RK (2003) Airflows and turbulent flux measurements in mountainous terrain: Part 1. Canopy and local effects. Agric For Meteorol 119(1–2), pp. 1–21, doi:10.1016/S0168-1923(03)00136-9

Webb EK, Pearman GI, Leuning R (1980) Correction of flux measurements for density effects due to heat and water vapour transfer. Q J R Meteorol Soc 106(447):85–100. doi:10.1002/qj.49710644707

Whiteman CD, Allwine KJ, Fritschen LJ, Orgill MM, Simpson JR (1989) Deep valley radiation and surface energy budget microclimates. Part I: Radiation. J Appl Meteorol 28(6):414–426

Wilson K, Goldstein A, Flage E, Aubinet M, Baldocchi D, Berbigier P, Bernhofer C, Ceulemans R, Dolman H, Field C, Grelle A, Ibrom A, Law BE, Kowalski A, Meyers T, Moncrieff J, Monson R, Oechel W, Tenhunen J, Sm Verma, Valentini R (2002) Energy balance closure at FLUXNET sites. Agric For Meteorol 113(1–4):223–243. doi:10.1016/S0168-1923(02)00109-0

Wohlfahrt G, Tasser E (2014) A mobile system for quantifying the spatial variability of the surface energy balance: design and application. Int J Biometeorol 59:617–627. doi:10.1007/s00484-014-0875-8

Zitouna-Chebbi R, Prévot L, Jacob F, Mougou R, Voltz M (2012) Assessing the consistency of eddy covariance measurements under conditions of sloping topography within a hilly agricultural catchment. Agric Forest Meteorol 164:123–135